Identification of a transcription factor-cyclin family genes network in lung adenocarcinoma through bioinformatics analysis and validation through RT-qPCR

XIAODONG YANG[1], YONGJIA ZHOU[2], HAIBO GE[2], ZHONGXIAN TIAN[3], PEIWEI LI[2] and XIAOGANG ZHAO[1,2]

[1]Department of Thoracic Surgery, The Second Hospital of Shandong University, Jinan, Shandong 250021; [2]Institute of Medical Sciences, Cheeloo College of Medicine, Shandong University, Jinan, Shandong 250100; [3]Key Laboratory of Chest Cancer, The Second Hospital of Shandong University, Jinan, Shandong 250021, P.R. China

Received April 21, 2022; Accepted August 30, 2022

DOI: 10.3892/etm.2022.11762

Abstract. Lung adenocarcinoma (LUAD) is the predominant pathological subtype of lung cancer, which is the most prevalent and lethal malignancy worldwide. Cyclins have been reported to regulate the physiology of various types of tumors by controlling cell cycle progression. However, the key roles and regulatory networks associated with the majority of the cyclin family members in LUAD remain unclear. In total, 556 differentially expressed genes were screened from the GSE33532, GSE40791 and GSE19188 mRNA microarray datasets by R software. Subsequently, protein-protein interaction network containing 499 nodes and 4,311 edges, in addition to a significant module containing 76 nodes and 2,631 edges, were extracted through the MCODE plug-in of Cytoscape. A total of four cyclin family genes [*cyclin* (*CCNA2*, *CCNB1*, *CCNB2* and *CCNE2*] were then found in this module. Further co-expression analysis and associated gene prediction revealed *forkhead box M1* (*FOXM1*), the common transcription factor of CCNB2, *CCNB1* and CCNA2. In addition, using GEPIA database, it was found that the high expression of these four genes were simultaneously associated with poorer prognosis in patients with LUAD. Experimentally, it was proved that these four hub genes were highly expressed in LUAD cell lines (Beas-2B and H1299) and LUAD tissues through qPCR, western blot analysis and immunohistochemical studies. The diagnostic value of these 4 hub genes in LUAD was analyzed by logistic regression, CCNA2 was deleted, following which a nomogram diagnostic model was constructed accordingly. The area under the curve values of CCNB1, CCNB2 and FOXM1 diagnostic models were calculated to be 0.92, 0.91 and 0.96 in the training set (Combined dataset of GSE33532, GSE40791 and GSE19188) and two validation sets (GSE10072 and GSE75037), respectively. To conclude, data from the present study suggested that the FOXM1/cyclin (CCNA2, CCNB1 and/or CCNB2) axis may serve a regulatory role in the development and prognosis of LUAD. Specifically, CCNB1, CCNB2 and FOXM1 have potential as diagnostic markers and/or therapeutic targets for LUAD treatment.

Correspondence to: Dr Peiwei Li, Institute of Medical Sciences, Cheeloo College of Medicine, Shandong University, 27 Shanda South Road, Jinan, Shandong 250100, P.R. China
E-mail: lipeiwei@email.sdu.edu.cn

Professor Xiaogang Zhao, Department of Thoracic Surgery, The Second Hospital of Shandong University, 247 Beiyuan Street, Jinan, Shandong 250021, P.R. China
E-mail: zhaoxiaogang@sdu.edu.cn

Key words: biomarker, lung adenocarcinoma, cyclins, gene expression, transcription factor, prognosis, nomogram, diagnostic

Introduction

Lung cancer is the most prevalent and lethal malignancy in the world, with lung adenocarcinoma (LUAD) being the predominant pathological subtype (1). Despite significant advances in early diagnostic and therapeutic approaches, the 5-year overall survival (OS) rate remains <20% (2). Platinum-based chemotherapy is currently the most important adjuvant therapy for patients with advanced lung cancer (3). However, adverse reactions and drug resistance limit the ultimate efficacy of chemotherapy (4). Therefore, novel strategies are in demand to supplement conventional therapeutic strategies (5). Over the past decade, knowledge on the molecular features of cancer has been steadily accumulating thanks to advances in genomic technology (6). Consequently, the preferred treatment strategy for advanced non-small cell lung cancer is shifting from traditional histopathology-based chemotherapy to individualized and precise treatment regimens based on oncogenic factors (7). Although the biomarkers and therapeutic targets previously identified have contributed to the diagnosis and treatment of LUAD, a demand remains for novel genetic data for optimizing treatment protocols due to its biological complexity and poor prognosis (8). To explore common biomarkers associated with cancer that can be used for treatment, diagnosis and assessment of prognosis, large quantities of cancer microarray and high-throughput

sequence data has been reported and become available over recent years (8,9). In addition, to overcome the limitations caused by small sample sizes, differential platform data and standards, bioinformatics are becoming increasingly popular in the field of cancer biology, which have yielded valuable information (8).

Cyclins are a class of proteins that control cell cycle progression by activating CDK enzymes (10). The cyclin gene family is comprised of 31 members according to the HUGO Gene Nomenclature Committee (https://www.genenames.org/data/genegroup/#!/group/473). Through bioinformatics technology, it was found that certain genes in certain cyclin families are significantly overexpressed in LUAD, but there is a lack of further experiments to verify their expression and specific molecular mechanisms (11). Although numerous studies have previously reported that cyclins serve important roles in the development of a variety of tumors (12,13), the specific genes in the cyclin family that are associated with the development of LUAD remain largely unexplored.

Based on the RNA microarray data of GSE33532, GSE40791 and GSE19188, the present study used bioinformatics methods to search for differentially expressed genes (DEGs) between LUAD and adjacent normal lung tissue. A protein-protein interaction (PPI) network was then established to screen for key genes enriched in the cyclin gene family. Online databases were implemented to validate the expression, PPI and clinical relevance of the hub genes. The purpose of the present study was to search for genes in the cyclin family that are associated with LUAD in addition to their potential upstream regulators. It is anticipated that this information could reveal potential targets for subsequent experimental validation.

Materials and methods

Microarray data source. In the present study, the microarray datasets were searched and downloaded from Gene Expression Omnibus (GEO) using the following criteria: i) Choose Affymetrix array under GPL570 platform; ii) the tissue source was from human LUAD samples and adjacent normal samples; and iii) study containing ≥20 LUAD and 20 normal samples. Finally, three datasets based on the GPL570 platform were selected, namely GSE19188, GSE33532 and GSE40791. Specifically, GSE19188 included 40 LUAD samples and 65 adjacent normal lung tissue samples (14), whereas GSE33532 included 40 LUAD samples and 20 adjacent normal lung tissue samples (15). GSE40791 included 94 LUAD samples and 100 adjacent normal lung tissue samples (16).

Microarray data analysis. The gene expression matrix and associated annotation files of the three aforementioned datasets were downloaded from the GEO database before the probe matrix in the expression profiling following the array was converted into a gene matrix through 'affy' package of R software (17). Under the R environment (version 4.0.3; https://www.r-project.org/), using the 'affy' package (17), the raw gene expression matrix was background corrected and normalized and the 'limma' package (18) was used to screen out the DEGs between the LUAD and normal samples $|\log_2$ fold change$|>1$ and $P<0.05$ were applied as the threshold for this screen.

Screening DEGs using robust rank aggregation (RRA) analysis. The RRA method is a tool that can be used for integrating data from multiple microarray studies with minimal inconsistencies to robustly identify DEGs (19,20). First, a list of the upregulated DEGs and downregulated DEGs by fold change in expression between the LUAD and normal samples was obtained from each dataset. Using the 'RRA' package (19), all lists of ranked genes from each dataset were integrated. Genes with an adjusted score <0.05 were significant DEGs.

Gene ontology (GO) and Kyoto encyclopedia of genes and genomes (KEGG) enrichment analysis. Enrichment analysis of GO and KEGG has been extensively utilized for deciphering microarray data to further understanding into the biological functions of each gene (21). In the present study, the 'ClusterProfiler' package (22) was used to analyze the GO and KEGG enrichment of the DEGs under the R environment (version 4.0.3).

PPI network establishment and module identification. Using the Search Tool for the Retrieval of Interacting Genes/Proteins (STRING; https://cn.string-db.org/, version 11.5) (23), a PPI network of DEGs was constructed to predict interactions among the proteins. A comprehensive score threshold ≥0.4 was considered to indicate a statistically significant interaction. In addition, the Cytoscape software (version 6.3; http://www.cytoscape.org/) (24) was used to further analyze and visualize the PPI network. Within Cytoscape, the 'NetworkAnalyzer' plugin was used to analyze the PPI network, whereas the 'MCODE' plugin was used to screen the functional module (25,26). The parameters set for screening the function module were as follows: MCODE score >5; degree cut-off=2; node score cut-off=0.2; Max depth=100; and k-score=2.

Screening for hub genes through co-expression and external databases. The enriched gene family was selected according to the gene module screened by Cytoscape. An expression correlation matrix was then made for the family genes in the three datasets, before genes with high positive correlation ($R>0.6$; $P<0.05$) were selected to be key genes according to Pearson's methods.

Subsequently, three datasets (GSE33532, GSE40791 and GSE19188) and the Gene Set Cancer Analysis (GSCA; http://bioinfo.life.hust.edu.cn/GSCA/#/) database were utilized to verify the expression of the key genes. The Gene Expression Profiling Interactive Analysis (GEPIA; http://gepia.cancer-pku.cn/index.html) database was used to assess the correlation in the expression of key genes, which genes that sufficiently correlate with each other ($R>0.7$; $P<0.001$) were selected as hub genes (27). The BioCarta (https://maayanlab.cloud/Harmonizome/) database was used to screen for the commonly predicted upstream transcription factors of the hub genes (28). Key genes in the cyclin family and their predicted upstream transcription factors were the ultimate hub genes of the present study.

Identifying and analyzing the hub genes. In the present study, the UALCAN database (http://ualcan.path.uab.edu/) (29) was used to compare the expression of hub genes in LUAD samples and normal samples, in addition to assessing the

association between the expression of hub genes and tumor stage and prognosis of patients with LUAD. In addition, the GEPIA database was used for the OS analysis of hub genes to explore their prognostic values (27).

Cells and cell culture. The LUAD cell line Beas-2B was cultured in high-glucose DMEM medium (cat. no. 23-10-013-CV; Corning, Inc.), the LUAD cell line A549 was cultured in high-glucose F12K medium (cat. no. 21127022; Thermo Fisher Scientific, Inc.), and the human bronchial epithelial cell line 16-HBE and LUAD cell line H1299 cell line were cultured in high-glucose RPMI-1640 medium (cat. no. 10-040-CV; Corning, Inc.). All mediums contained 10% FBS (cat. no. 10091148; Gibco; Thermo Fisher Scientific, Inc.), 100 U/ml penicillin and 100 μg/ml streptomycin and cells were incubated routinely in a cell incubator containing 5% CO_2 at 37˚C. The three cell lines were purchased from FuHeng Cell Center (https://www.fudancell.com/). Cells at logarithmic growth phrases were used for subsequent experiments.

Reverse transcription-quantitative PCR (RT-qPCR). According to the manufacturer's protocol, the TRIzol® reagent (cat. no. 15596026; Invitrogen; Thermo Fisher Scientific, Inc.) to isolate total RNA from the 16-HBE, A549, Beas-2B and H1299 cells. Reverse transcription was performed using super script first strand synthesis system cat. no. 18080051; Invitrogen; Thermo Fisher Scientific, Inc.) with oligo (DT) 20 primer and 5.0 μg RNA to synthesize the first strand of cDNA. Using GAPDH as the endogenous control, the primers were synthesized by Beijing Tsingke Biotechnology Co., Ltd. Primer sequences are provided in Table SI. Master qPCR mix (2X TSINGKE® SYBR Green I; cat. no. 4367659; Invitrogen; Thermo Fisher Scientific, Inc.) was used to detect mRNAs level according to the manufacturer's protocol (initial denaturation: 95˚C for 3 min; followed by 40 cycles of denaturation at 95˚C for 10 sec, annealing at 55˚C for 10 sec and extension at 72˚C for 30 sec.). Application of the $2^{-\Delta\Delta Cq}$ method was used to calculate the relative expression level of mRNA (30).

Western blot analysis. The protein samples lysate for western blot were collected from 16-HBE, Beas-2B, A549 and H1299 cell lines with RIPA lysis buffer (cat. no. P0013B; Beyotime Institute of Biotechnology) containing protease inhibitor cocktail. Concentrations of protein samples were detected using the BCA Protein Assay Kit (cat. no. A53225; Thermo Fisher Scientific, Inc.) and 20 μg protein lysate was loaded in 10% SDS-PAGE gel respectively and transferred to PVDF membrane (Bio-Rad Laboratories, Inc.). After blocking in 5% non-fat milk dissolved in TBST buffer for 60 min at room temperature, the membranes were washed 3 times by TBST containing 1% Tween 20 (cat. no. P1379; Sigma-Aldrich; Merck KGaA) and then incubated with the following 5% BSA-diluted (cat. no. ST2254; Beyotime Institute of Biotechnology) primary antibodies: CCNA2 (1:1,000; cat. no. 18202-1-AP), CCNB1 (1:1,000; cat. 28603-1-AP), CCNB2 (1:1,000; cat. no. 21644-1-AP; all from ProteinTech Group, Inc.) and ACTB (1:10,000; cat. no. AC026; Abclonal Biotech Co., Ltd.) for 6-8 h at 4˚C; the HRP-linked secondary antibodies (1:20,000; cat. no. SA00001-2; ProteinTech Group, Inc.) were used to probe the primary antibodies for 1 h at room temperature. Finally, the immunoreactive protein bands were visualized by ECL kit (cat. no. WBKLS0500; MilliporeSigma), and the images were obtained by scanning using a fluorescence imager (Typhoon FLA 7000; Cytiva). The quantification of blot bands was calculated using ImageJ (Version. 1.52; National Institutes of Health).

Immunohistochemistry of hub genes. In total, 10 pairs of LUAD and adjacent normal tissues were collected from the Second Hospital of Shandong University (Jinan, China) from 2021/01/01 to 2021/12/31, with complete pathological data. The age of the patients was 61.2±6.3 years, including 4 women and 6 men. The present study was approved [approval no. KYLL-2020(KJ)P-0099] by the Medical Ethics Committee of the Second Hospital of Shandong University (Jinan, China). Written informed consent was obtained from all participants. The human LUAD specimens were formalin-fixed and paraffin-embedded for 24 h at 4˚C and cut into 4-μm thin slices. The IHC staining kit (cat. no. PV-6000; ZSGB-BIO) was used for the experiment according to the manufacturer's instructions. DAB (cat. no. ZLI-9017; ZSGB-BIO) was used for staining (37˚C for 90 sec). The final immunostaining images were obtained using a NanoZoomer Digital Pathology scanner (NanoZoomer S60; Hamamatsu Photonics K.K.). Protein expression was analyzed by calculating the integrated optical density (IOD/area) of each stained region using Image-Pro Plus version 6.0 (Media Cybernetics, Inc.).

Diagnostic model and evaluation of hub genes. To evaluate the diagnostic efficacy of the hub genes for LUAD, the three data sets GSE33532, GSE40791 and GSE19188 were combined. The raw expression data were then normalized by Affy package (17) using robust multi-array average (RMA), before the inter-batch differences were removed and the data were integrated into a large expression matrix. The percentage of normal tissue in all samples was calculated, and the cut-off value was selected according to the percentage of normal tissue in the sample. Those whose expression value was higher than the cut-off value were regarded as high expression samples, and those whose expression value was lower than the cut-off value were regarded as low expression samples. The expression of samples was converted from numerical variables to factor variables for subsequent analysis. This integrated expression matrix was used as the training set. To verify the diagnostic efficacy, two external datasets were also selected, namely GSE10072 (31) and GSE75037 (32) for external data validation. GSE10072 belongs to the same GPL570 platform as the three datasets used for the training set. The raw data of GSE10072 were analyzed after RMA normalization. By contrast, the GSE75037 dataset belongs to the GPL6884 platform. To verify the applicability of the data from other platforms, the matrix expression data from this dataset were chosen for analysis. The training set contains 179 LUAD samples and 185 normal tissue samples in total. The external validation set GSE10072 contains 58 LUAD samples and 49 normal tissue samples. The external validation set GSE75037 contains 83 LUAD samples and 83 normal tissue samples.

MASS package (33) and glm function (34) were used for forward stepwise logistic regression analysis of hub gene, and the appropriate genes were selected and included into

the effect variables. Then glm function was used to conduct logistic regression analysis on the key genes included in the effect variables. Finally, rms package (35) was used to construct nomograph of regression analysis results.

A ROC curve for this model was constructed using the 'pROC package' (36). ROC curves were generated for the training set and two validation sets to distinguish patients with LUAD from healthy individuals. Area under the ROC curve (AUC) and confidence intervals were calculated to assess the predictive values of the selected hub genes for LUAD diagnosis. Finally, the diagnostic efficacy of the nomograms was evaluated further and validated using calibration plots and decision curve analysis (DCA) plots through rms package (35).

Statistical analysis. Statistical comparisons were performed using SPSS 25.0 (IBM Corp.). The Pearson correlation coefficient between cyclin family genes was calculated using R (https://www.R-project.org/). In the GEPIA database, Pearson's method was used to analyze the expression correlation between hub genes in TCGA datasets. GEPIA used the Kaplan-Meier method to estimate the OS associated with gene expression levels. GEPIA uses the Mantel-Cox test for hypothesis testing. The cox proportional hazard ratio and the 95% confidence interval information are shown in the survival plot. One-way ANOVA was used to analyze whether the results of western blotting and RT-qPCR were statistically different. In the multiple comparisons post hoc test, Dunnett's test was used to compare the non-small cell lung cancer cell lines A549, Beas-2B and H1299 with the control cell line 16-HBE, respectively. In the results of immunohistochemical study, paired t-test was used to analyze whether the staining results of hub gene in normal adjacent tissues and tumor tissues were statistically different. The significance of the difference between the two groups was estimated by UALCAN using the t-test, but the statistical analysis method used for the comparison of multiple groups was not described. $P<0.05$ was considered to indicate a statistically significant difference.

Results

Analysis of LUAD microarray data. In the present study, GSE19188, GSE33532 and GSE40791 were included for analysis, with a total of 179 LUAD samples and 185 normal samples. These three microarray datasets were first standardized by quantiles to mitigate individual differences among samples. A total of 1,883, 3,079 and 2,258 DEGs were screened from the GSE19188, GSE33532 and GSE40791 datasets, respectively (Fig. 1A-C).

RRA-integrated analysis and identification of DEGs. The RRA method assumes that the number of ranked each gene is known (19). The smaller the RRA score, the higher the gene ranks in term of the credibility of differential expression. Finally, 556 significant DEGs were screened by the integrated analysis, including 203 significantly upregulated genes and 353 significantly downregulated genes. A heatmap containing the top 10 up- and downregulated genes is shown in Fig. 1D.

Functional and pathway enrichment analysis of the DEGs. GO analysis revealed that biological processes of the significant DEGs were associated with the cell cycle, including 'mitotic nuclear division', 'extracellular matrix organization', 'extracellular structure organization', 'mitotic sister chromatid segregation' and 'chromosome segregation' (Fig. 2A). Significantly enriched cellular components included 'collagen-containing extracellular matrix', 'condensed chromosome' and 'centromeric region' (Fig. 2B). In addition, the molecular functions that were significantly enriched include 'extracellular matrix structural constituent', 'glycosaminoglycan binding' and 'growth factor binding' (Fig. 2C). KEGG analysis revealed that DEGs were significantly enriched in 'ECM-receptor interaction', 'protein digestion and absorption', 'cell cycle' and 'cell adhesion molecules' (Fig. 2D).

PPI network of DEGs and module identification. A total of 499 nodes and 4,311 edges were found in the PPI network (Fig. 3A). Using the 'Networkanalyzer' plugin, the basic parameters of the PPI network were obtained, where the clustering coefficient was 0.342, the network density was 0.035 and the network centralization was 0.147. Using the Cytoscape plugin 'MCODE', the most critical module was acquired from the PPI network, which contains 76 nodes and 2631 edges (Fig. 3B). The most significantly enriched pathway for module 1 is cell cycle (Fig. 3C).

Screening for key genes in the cyclin family. A total of four cyclin family genes (CCNA2, CCNB1, CCNB2 and CCNE2) were clustered in module 1. To analyze the cyclin family genes, a cyclin family gene expression correlation matrix was made for the three datasets. The results revealed that *CCNE1*, *CCNE2*, *CCNB1*, *CCNB2*, *CCNA2* and *CCNF* correlated with each other (Fig. 4A-C). The expression of six cyclin family genes was then analyzed in the three datasets: CCNE1, CCNE2, CCNB1, CCNB2 and CCNA2 were all highly expressed in the three data sets, while CCNF was only highly expressed in GSE33532, while there was no significant difference in the other two data sets (Fig. 4D). The expression profile of *CCNE1*, *CCNE2*, *CCNB1*, *CCNB2*, *CCNA2* and *CCNF* was subsequently analyzed in various tumors using the GSCA database. It was found that the expression of most if not all the genes examined were upregulated in multiple human tumors, including LUAD, breast and colon cancer (Fig. 4E).

Analysis of hub gene co-expression. To investigate the correlation in the expression of the six cyclin family genes, the GEPIA online tool was used to obtain the Pearson's rank coefficient results among these genes. According to the pairwise gene expression correlation analysis, GEPIA revealed significant positive correlation among *CCNB1*, *CCNB2* and *CCNA2* expression (Fig. 5A-C). The BioCarta database was next used to screen for possible upstream transcription factors of *CCNB2*, *CCNB1* and *CCNA2*. *FOXM1* was predicted to be their common upstream transcription factor. In addition, *FOXM1* was also found to be an upregulated gene clustered in module 1 (Fig. 3B). According to the GEPIA database, *FOXM1* also appeared to be a co-expressed gene with the three cyclins (Fig. 5D-F). Therefore, these four genes were chosen to be hub genes for further verification.

Expression of hub genes and their prognostic value. The UALCAN database is based on The Cancer Genome Atlas data (29). Therefore, this online tool was used to assess the

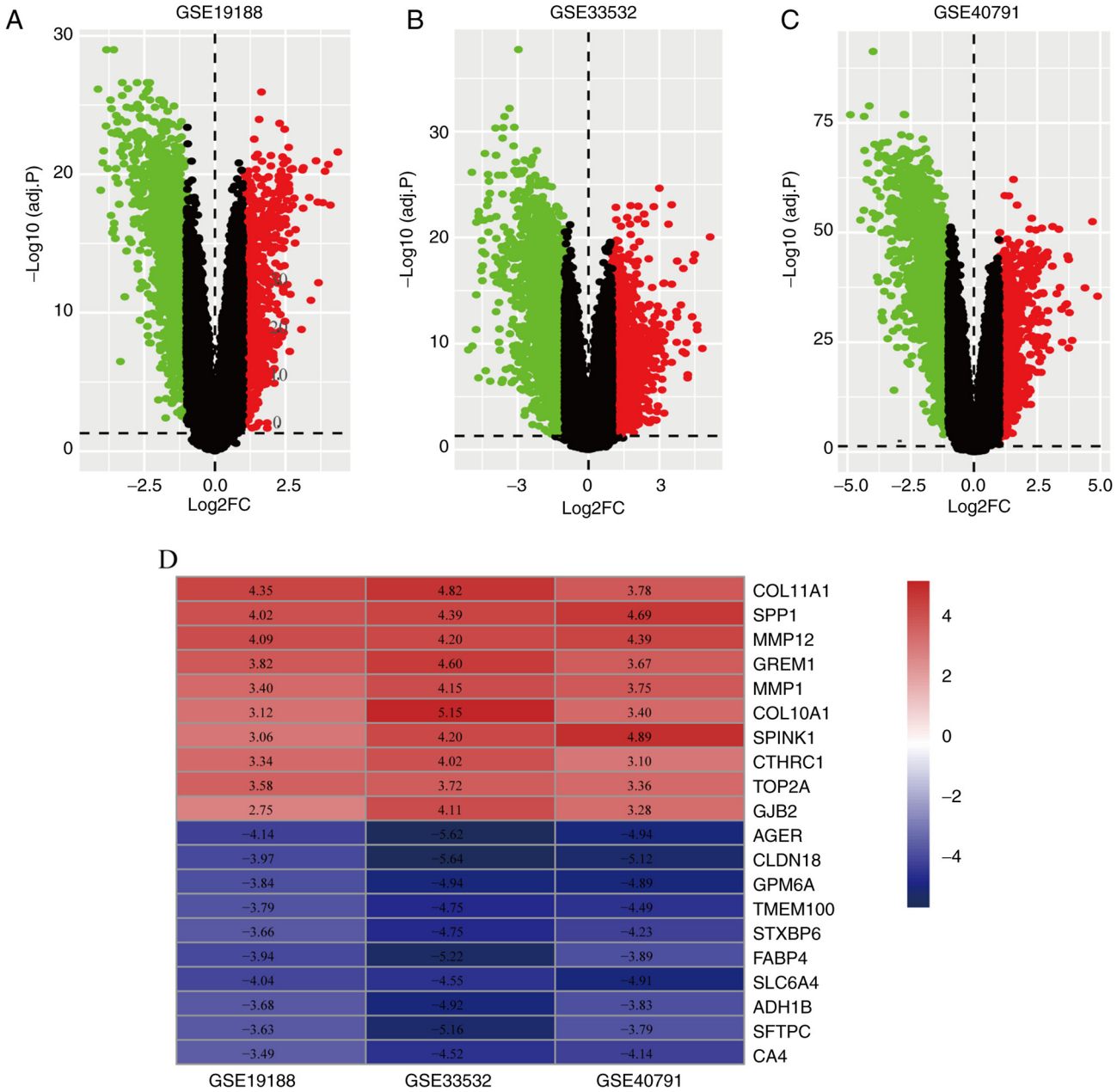

Figure 1. Volcano plots of the three microarray datasets. Differentially expressed genes of LUAD and normal samples in (A) GSE19188, (B) GSE33532 and (C) GSE40791. Red points represent upregulated genes, whilst green points represent downregulated genes. Black points represent genes with no significant difference in expression. (D) Heatmap of the top 10 up- and downregulated genes according to robust rank aggregation analysis. Red and blue represent genes with higher and lower expression levels in patients with LUAD, respectively. LUAD, lung adenocarcinoma.

expression profile of the hub genes. The expression of these hub genes was found to be higher in the LUAD samples compared with that in the normal samples (Fig. 6A-D). The association between hub gene expression and tumor stage was next assessed (Fig. 6E-H). All four hub genes were revealed to be expressed in tumors of different stages, but the levels were higher in advanced LUAD compared with those in their early-stage counterparts. The GEPIA website was next used to assess the prognostic value of these hub genes in the clinical setting, where a total of 240 patients with LUAD were included from the database available for overall survival (OS) analysis. Higher expression of all these hub genes was associated with more unfavorable OS among patients with LUAD (Fig. 6I-L).

Validation of hub gene expression in vitro. RT-qPCR was used to verify the mRNA expression levels of these genes in the cell lines. The results showed that the mRNA expression of the hub genes was significantly higher in the two non-small cell lung cancer cell lines Beas-2B and H1299 compared with human bronchial epithelial cell line 16-HBE, and the expression of four hub genes was upregulated in A549 cell line, in which there was a significantly high expression in CCNB1 and CCNB2 (Fig. 7A-D, Tables SII-V). Subsequently, western blotting revealed that the CCNA2, CCNB1 and CCNB2 were also highly expressed in the three non-small cell lung cancer cell lines A549, Beas-2B and H1299 compared with human bronchial epithelial cell line 16-HBE (Fig. 7E, Tables SVI-VIII). According to the immunohistochemistry staining images of the hub genes in 10 pairs of

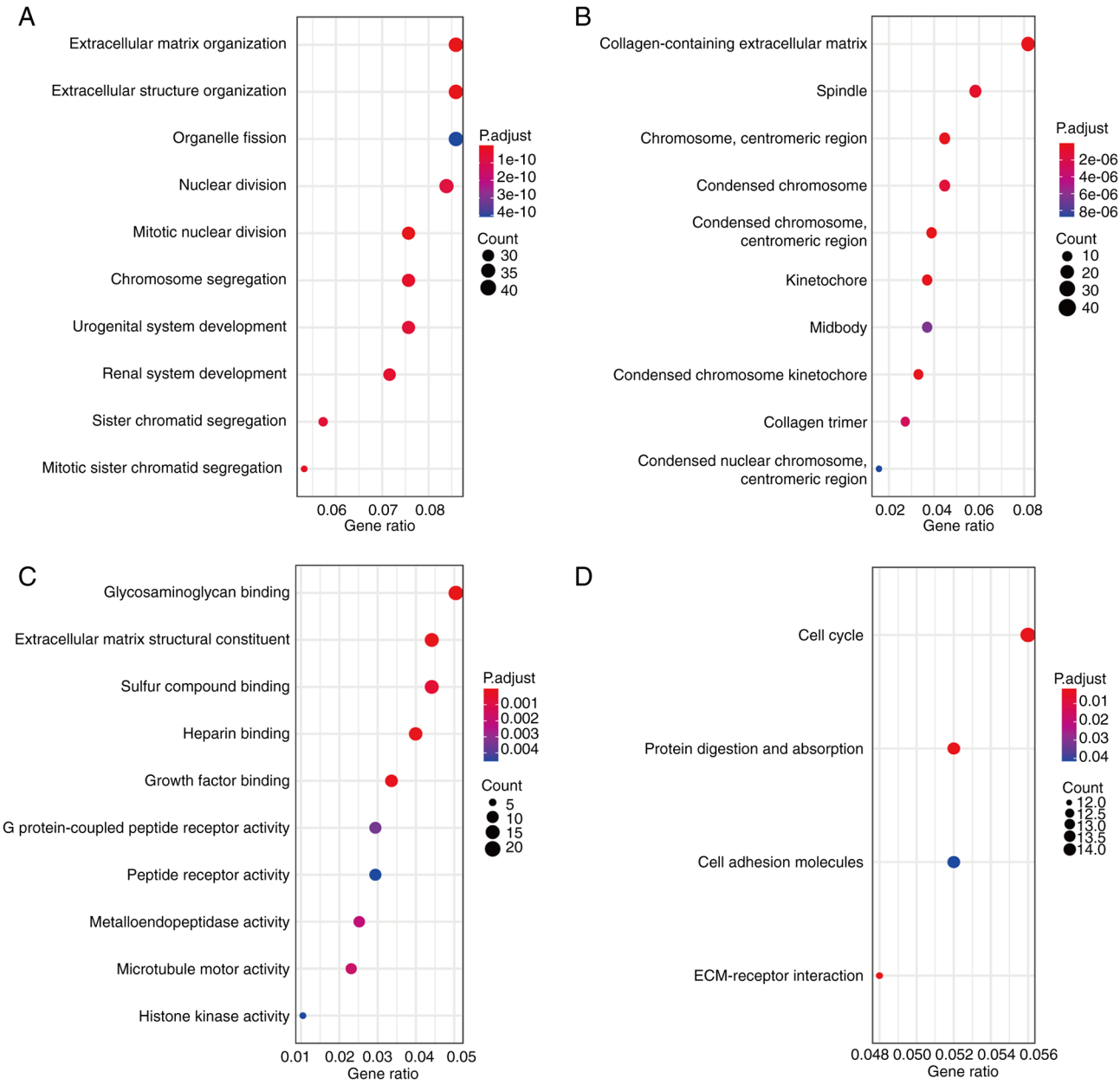

Figure 2. GO and pathway enrichment analysis of differentially expressed genes in lung adenocarcinoma. Top 10 GO terms in (A) biological processes, (B) cellular components, (C) molecular function and (D) Kyoto Encyclopedia of Genes and Genomes pathways. GO, gene ontology.

human LUAD tissues and adjacent normal tissues, their expression in tumors was found to be significantly higher compared with that in the adjacent normal tissues (Fig. 7F-G).

Diagnostic model and evaluation of hub genes. The diagnostic efficacy of all hub genes was assessed by constructing multi-factorial logistic regression models from the training set, where *CCNB1*, *CCNB2* and *FOXM1* were statistically significant (Table SIX). *CCNB1*, *CCNB2* and *FOXM1* were analyzed further after their inclusion as possible effect variables (Table SX). All hub genes were found to be statistically significant.

Since the expression levels of *CCNB1*, *CCNB2* and *FOXM1* appeared to be predictors of LUAD, the nomogram plots were constructed to assess their diagnostic efficacy (Fig. 8A). ROC analysis was subsequently applied to evaluate the potential diagnostic value of these hub genes in LUAD. The results showed that *CCNB1*, *CCNB2* and *FOXM1* had AUC values of 0.92 (95% confidence interval=0.89-0.95) in the training set, 0.91 (95% confidence interval=0.86-0.97) in the GSE10072 validation set for the diagnosis of LUAD and 0.96 (95% confidence interval=0.93-0.99) in the GSE75037 validation set (Fig. 8B). This suggested that *CCNB1*, *CCNB2* and *FOXM1* are viable biomarkers for LUAD diagnosis (Fig. 8B). The calibration plot also revealed consistent predictive accuracy for the diagnosis of LUAD using the hub genes (Fig. 8C). DCA plot results revealed that clinical benefit could be obtained by developing clinical strategies based on this nomogram (Fig. 8D).

Discussion

Dysregulation in cell cycle control can lead to tumor progression. Cyclins are cell cycle regulators that are associated with

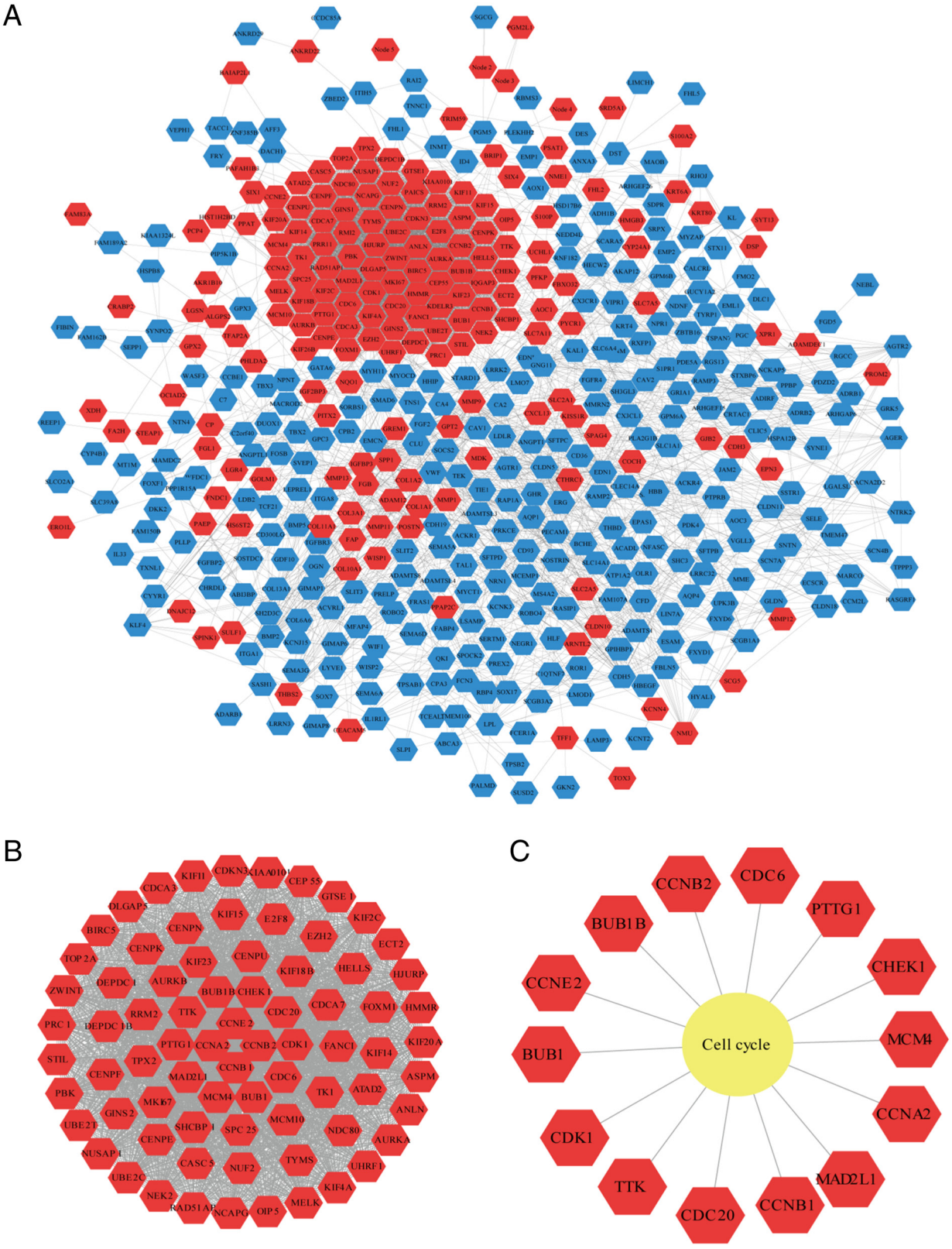

Figure 3. PPI network and the most significant module formed by the DEGs in lung adenocarcinoma. (A) PPI network of DEGs. (B) The most significant module from the PPI network, containing 76 differentially expressed genes. (C) The most significantly enriched pathway for module 1. Red represents genes with higher expression levels, whilst blue represents genes with lower expression levels. Yellow representσ the pathway of the cell circle. PPI, protein-protein interaction; DEGs, differentially expressed genes.

numerous types of cancer (12,13). However, it remains unclear the role and possible regulatory mechanism of cyclins in LUAD.

In the present study, expression profiling and functional enrichment analysis revealed that four significant DEGs, namely *CCNA2*, *CCNB1*, *CCNB2* and *CCNE2*, were highly

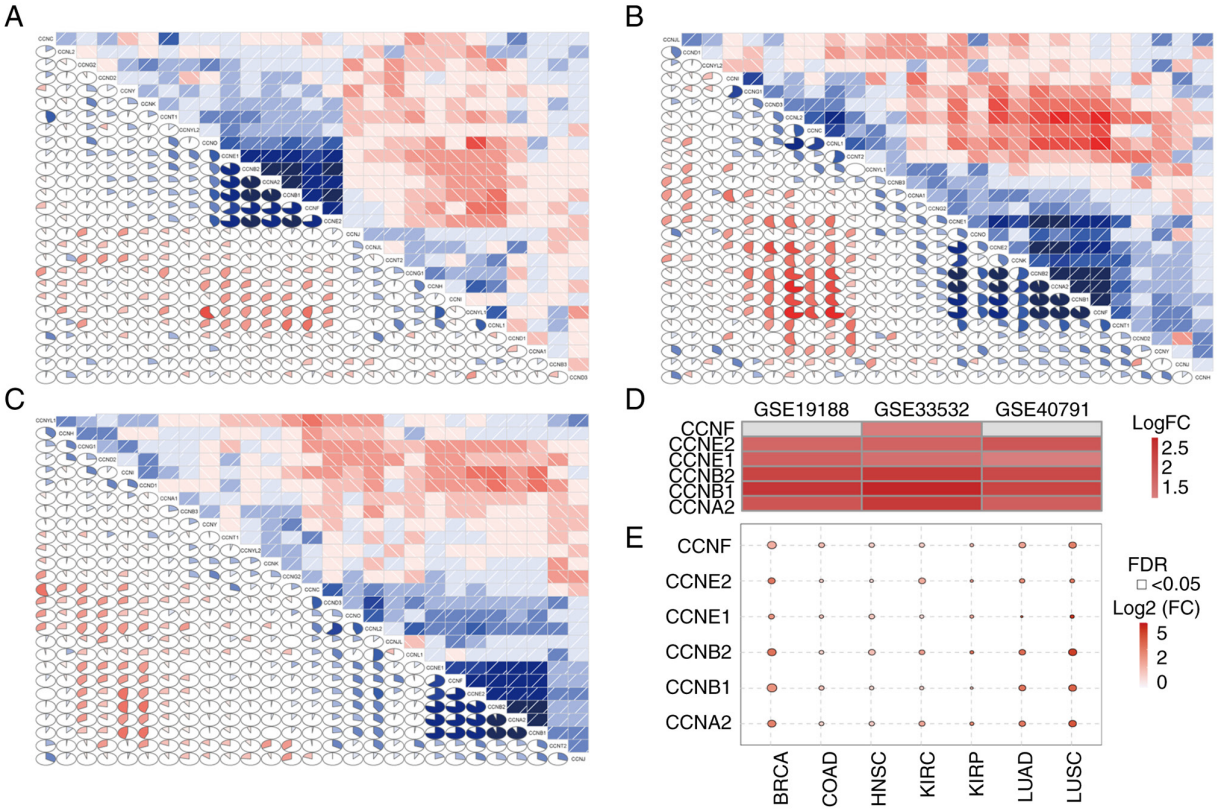

Figure 4. Cyclin family gene expression profile. Correlation matrix of the expression levels of all genes in the cyclin family in the (A) GSE19188, (B) GSE33532 and (C) GSE40791 datasets. (D) Expression of sex cyclin family genes (*CCNE1*, *CCNE2*, *CCNB1*, *CCNB2*, *CCNA2* and *CCNF*) in the three datasets. (E) Expression of sex cyclin family genes in various tumors according to the Gene Set Cancer Analysis database. BRCA, breast invasive carcinoma; COAD, colon adenocarcinoma; HNSC, head and neck squamous cell carcinoma; KIRC, kidney renal clear cell carcinoma; KIRP, kidney renal papillary cell carcinoma; LUAD, lung adenocarcinoma; LUSC, lung squamous cell carcinoma.

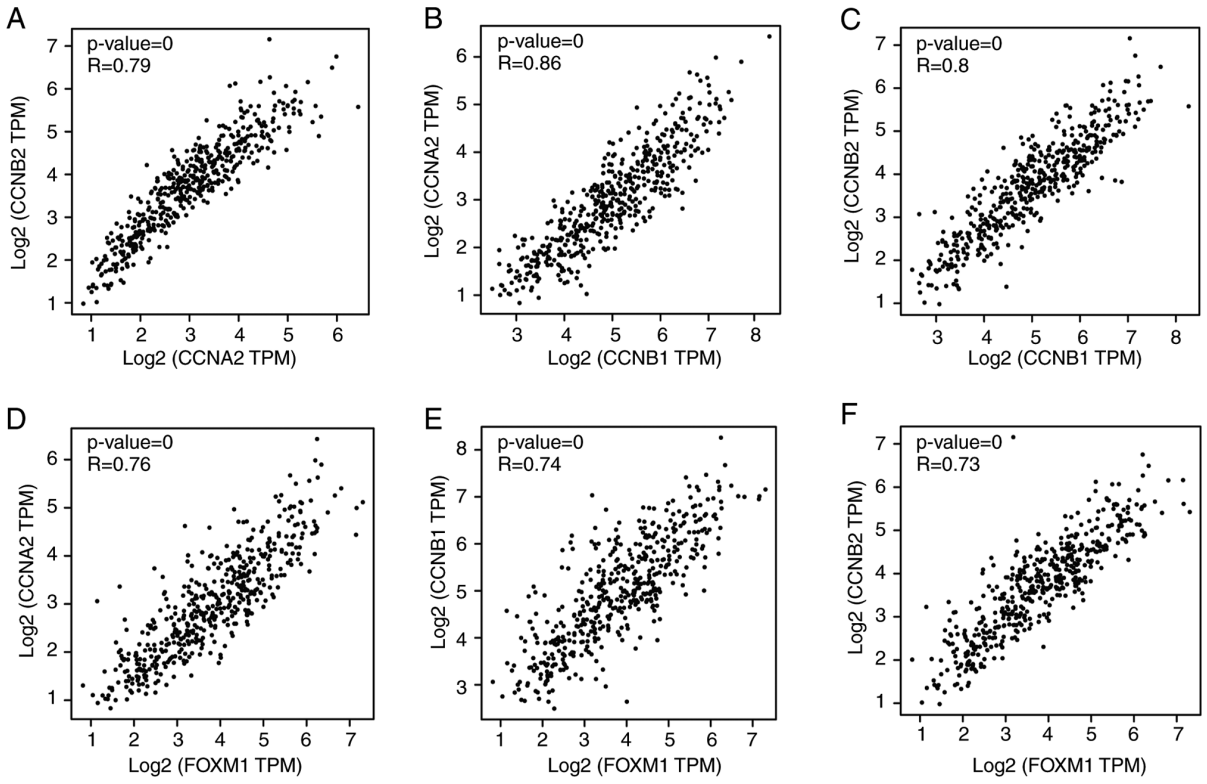

Figure 5. Correlation in the expression of the hub genes. Correlations between (A) CCNB2-CCNA2, (B) CCNB1-CCNA2 and (C) CCNB1-CCNB2 are significant (R>0.75; P<0.001). Correlation between Forkhead box M1 and (D) CCNA2, (E) CCNB1 and (F) CCNB2 in lung adenocarcinoma was revealed by GEPIA (R=0.76, 0.74 and 0.73 respectively). CCN, cyclin.

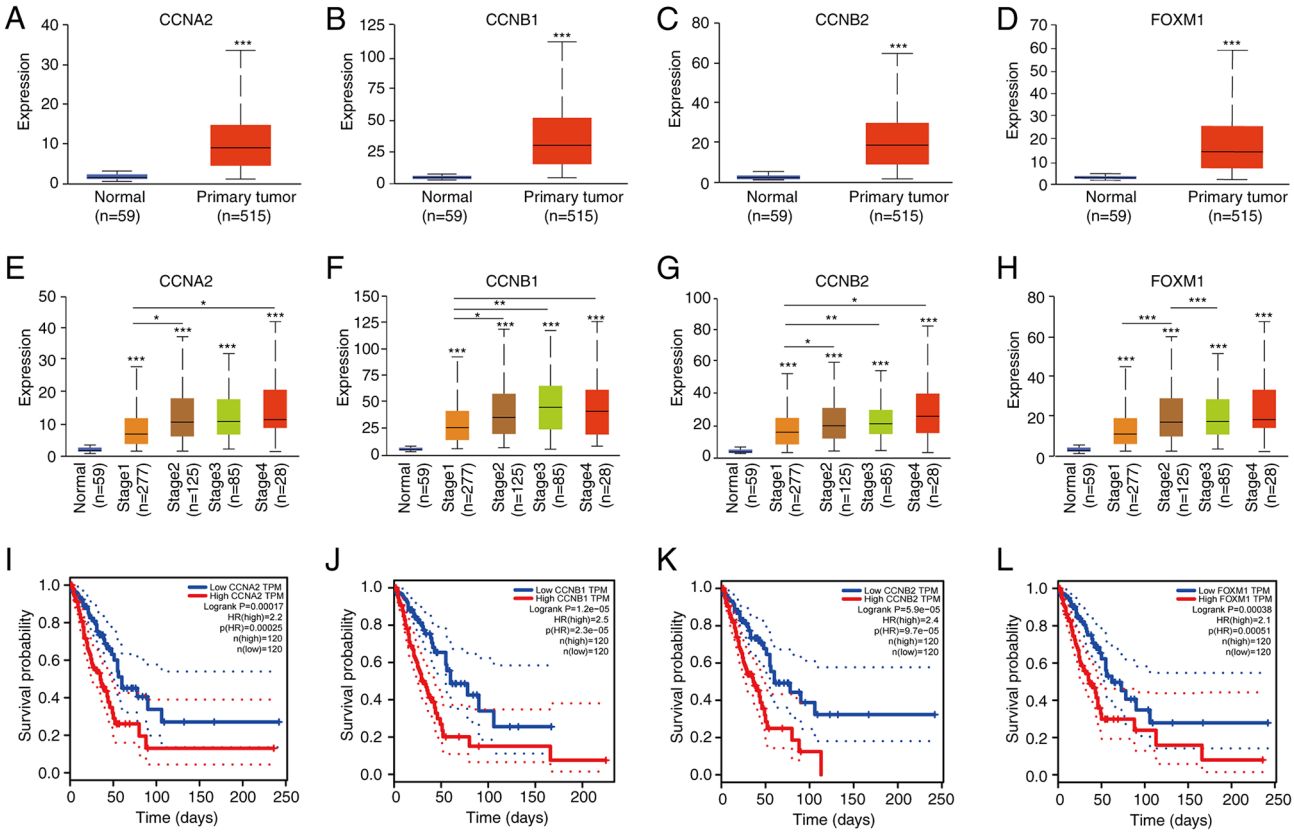

Figure 6. Expression levels of hub genes and patient prognosis. (A-D) Identifying the expression levels of the hub genes in LUAD using UALCAN. (E-H) Association between hub gene expression and adenocarcinoma tumor stage. (I-L) Survival curves comparing the prognosis of patients with high and low expression levels of hub genes in LUAD according to the GEPIA database. *P<0.05, **P<0.01 and ***P<0.001. LUAD, lung adenocarcinoma.

expressed in module 1. An expression correlation matrix containing 31 cyclin family genes in three datasets also showed that six genes (*CCNE1*, *CCNE2*, *CCNB1*, *CCNB2*, *CCNA2* and *CCNF*) are significantly co-expressed. Further analysis of their expression in the datasets and pan-tumor data demonstrated that they were significantly overexpressed in a variety of tumors, such as breast cancer and colon cancer. Further co-expression analysis also revealed that the correlation among the expression levels of *CCNA2*, *CCNB1* and *CCNB2* was particularly striking. In addition, *FOXM1* was predicted to be their upstream transcription factor according to the BioCarta database, where the co-expression results reported significant co-expression between *FOXM1* and the three cyclin family genes. Since further study revealed that FOXM1 was also enriched in module 1, it was included as one of the hub genes for further analysis and validation.

Using online databases, the high expression of hub genes was found in LUAD. Furthermore, the expression of *CCNA2*, *CCNB1*, *CCNB2* and *FOXM1* was found to be higher in patients with advanced LUAD compared with that with early-stage LUAD. Kaplan-Meier analysis revealed that patients with higher levels of hub gene expression had poorer prognoses, suggesting that they are viable prognostic indicators of LUAD. In terms of biological function, the hub genes were enriched in the cell cycle, DNA damage, DNA repair, invasion and proliferation according to the single-cell pan-tumor function enrichment study. These results may provide phenotypic directions for further experimental verification. On protein level, results from immunohistochemical analysis also confirmed the higher protein expression levels of hub genes in LUAD compared with those in normal tissues. To validate the results on a cellular level, the mRNA and protein expression of these hub genes were found to be upregulated in the cancer cell lines Beas-2B and H1299 compared with those in the control cell line 16-HBE. Immunohistochemistry results also showed that the hub genes are expressed highly in LUAD tissues.

The protein encoded by *CCNB1* is a mitosis-associated regulatory protein (37). It functions as a controller of mitosis entry (38). CCNB1 recombines with Cdk1, which divides the nuclear envelope to allow the mitotic spindle to enter the chromosome. The role of CCNB1 is to facilitate entry from the G_2 phase to the M phase (39). CCNB1 overexpression can lead to uncontrolled cell proliferation by binding Cdk1 (40). Previous studies have shown that the expression level of CCNB1 was increased in a variety of solid tumors, including breast and colorectal, where the survival rate of patients with cancer with higher CCNB1 expression was lower (41). In pituitary adenomas, the upregulated CCNB1 expression has been reported to serve an important role in the pathological development of the disease, suggesting that it can be used as a marker to evaluate tumor invasiveness (42). In another study, Chen *et al* (43) previously revealed that higher expression levels of CCNB1 promoted the proliferation, migration and invasion of gastric cancer cells (43). In terms of the mechanism, inhibiting the expression of CCNB1 can inhibit the proliferation of pancreatic cancer cells through the p53 signaling pathway (44).

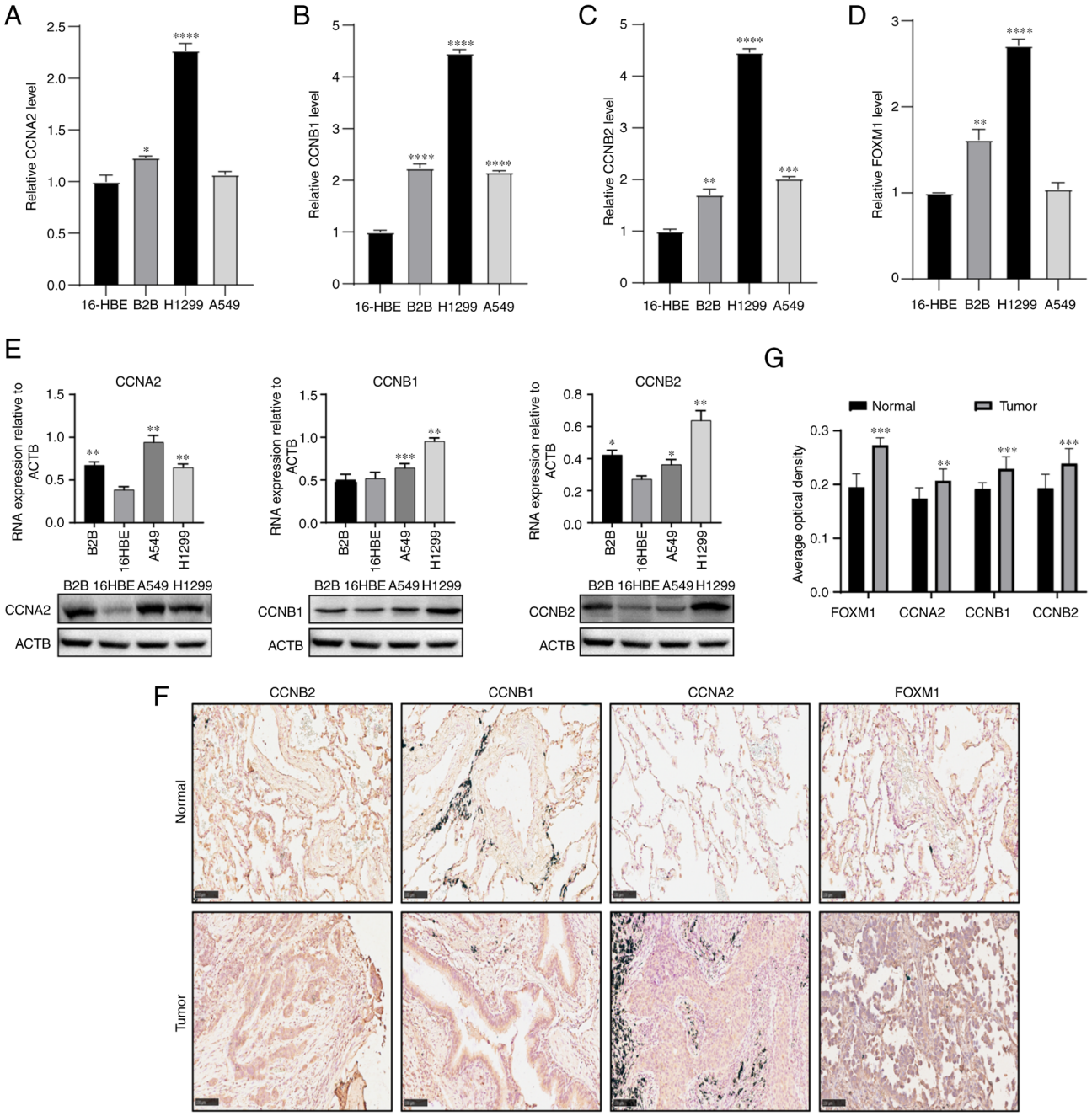

Figure 7. Expression of hub genes in LUAD cells and tissues. The expression levels of (A) CCNA2, (B) CCNB1, (C) CCNB2 and (D) FOXM1 mRNA in the non-small cell lung cancer cell lines A549, Beas-2B and H1299 and the control cell line 16-HBE were validated by reverse transcription-quantitative PCR. (E) Western blot analysis was used to detect the expression of CCNA2, CCNB1 and CCNB2 in LUAD cell lines; ACTB was used as loading control. Each column represents the mean ± SD from independent experiment. (F) Immunohistochemistry was used to analyze the expression of hub genes in LUAD and adjacent normal tissues (magnification, x200; scale bar, 100 μm). (G) Image-Pro Plus version 6.0 was used to calculate the integral optical density/area and analyze the hub gene protein expression level. Statistical analysis of results in panels A-E was performed using one-way ANOVA, and comparisons between groups were performed using Dunnett's test. Statistical analysis of results in panel F was performed using t-test. *P<0.05, **P<0.01, ***P<0.001 and ****P<0.0001 compared with 16-HBE. LUAD, lung adenocarcinoma; CCN, cyclin.

CCNB2 is a B-type cyclin (45). Qian *et al* (46) previously found that the higher expression of CCNB2 is associated with the progression and poor prognosis of non-small-cell lung cancer (46). In addition, CCNB2 has been reported to be expressed highly in bladder cancer, where inhibiting CCNB2 expression can inhibit tumor invasion and metastasis (47). CCNB2 was also revealed to affect the CCNB2/polo-like kinase pathway to promote cell proliferation and migration in hepatocellular carcinoma (48). In another recent study, Wang *et al* (49) found that microRNA-335-5p may be a negative upstream regulator of CCNB2 to inhibit the proliferation of LUAD cells.

CCNA2 belongs to a highly conserved cyclin family (50). CCNA2 has been found to be expressed highly in pancreatic cancer, where its expression levels were positively associated with tumor stage and poorer prognosis (51). In non-small-cell lung cancer, higher expression levels of CCNA2 have been proposed to be a biomarker of poor prognosis (52). In

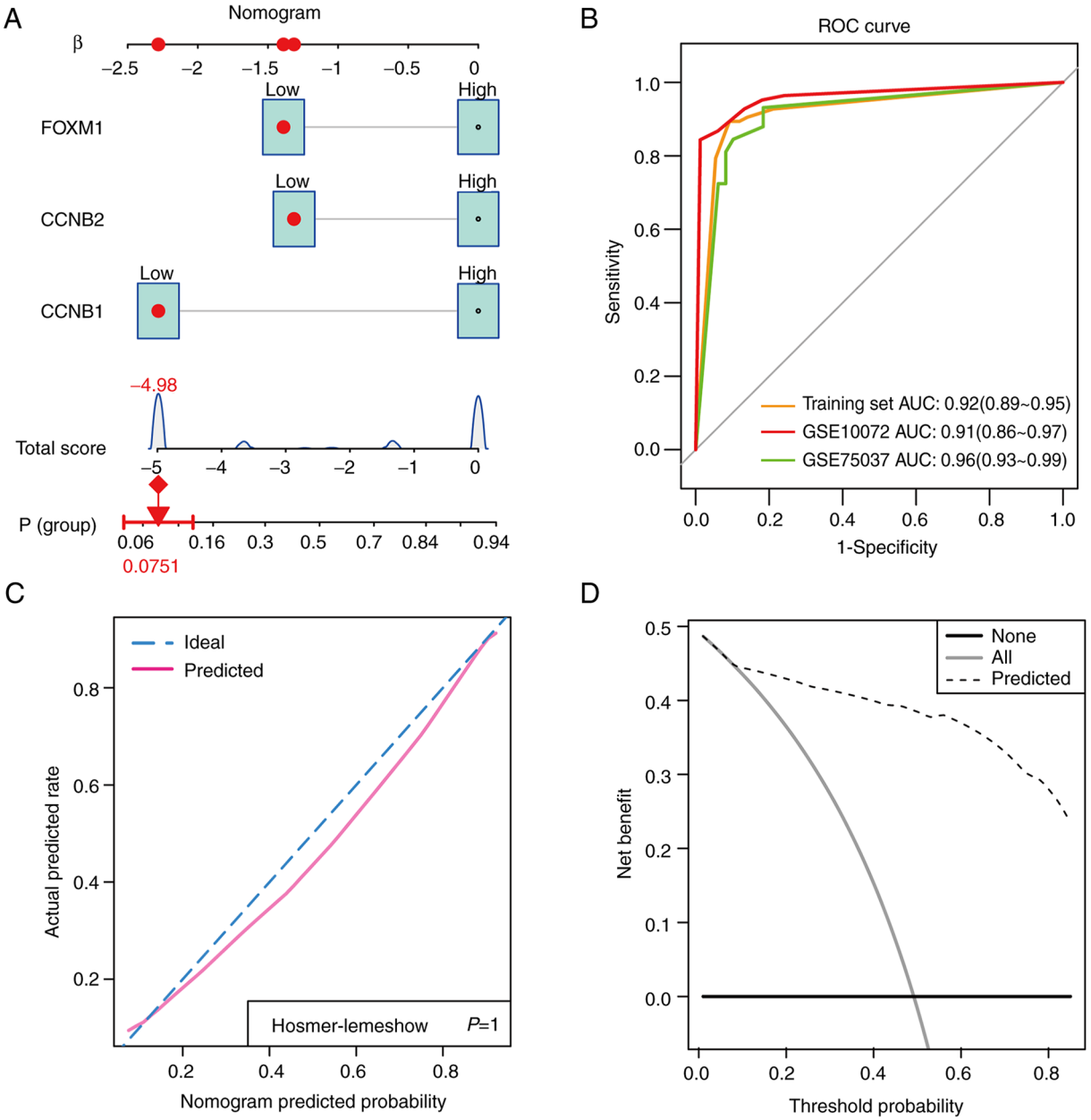

Figure 8. Nomogram construction and evaluation. (A) Nomogram constructed using CCNB1, CCNB2 and FOXM1 expression. Red dots represent the outcome values of one of the samples and the predicted results in the Nomogram. (B) Receiver operating characteristic curves and area under the curve values of the diagnostic model in the training set (yellow line), validation set GSE10072 (green line) and the validation set GSE75037 (red line). (C) Calibration curves for the nomogram, where the prediction curves were close to the ideal curve and the Hosmer-Lemeshow test was ~1, suggesting consistency for the detection of lung adenocarcinoma for the hub genes used. (D) Decision curve analysis graph. The gray line represents the hypothesis that all lesions are malignant (full treatment option). The solid black line represents the hypothesis that all lesions are benign (no treatment option). The black dashed line represents the decision to treat benign or malignant based on the fitted model. The results show that using the nomogram designed to predict malignancy increases the benefit of developing a treatment plan over treating all (gray solid line) or no treatment (black solid line).

addition, higher expression of CCNA2 in patients with stage I non-small-cell lung cancer may indicate a worse prognosis and higher recurrence rates (53). Mechanistically, tanshinone has been shown to inhibit the progression of LUAD by regulating the expression of CCNA2 (54). Several bioinformatics studies also previously revealed that CCNA2 is a potential therapeutic target and prognostic marker of breast and gastric tumors (55,56).

FOXM1 is a member of the FOX transcription factor family that serves an important role in cell proliferation, differentiation and survival (57,58). Several studies have shown that higher expression levels of FOXM1 are closely associated with poorer prognosis in small cell lung cancer (58,59). In terms of mechanism, FOXM1 can regulate cell cycle progression and improve the invasiveness of bladder cancer (60). Furthermore, FOXM1 can be indirectly recruited to the homologous region element of the cell cycle gene through the Myb-MuvB complex, which enables it to specifically control the expression of *CCNB1* and *CCNB2* during the G_2/M phase of the cell cycle (61). A previous study showed that higher expression of FOXM1 can increase the expression of CCNB1, where FOXM1 mainly mediates its biological function through inhibiting the activation of the p53

pathway by recruiting CBP/P300 (62). Chai *et al* (63) previously found that the FOXM1/CCNB1 axis can promote the proliferation of liver cancer cells, which can be reversed by blocking this axis.

Nomograms have been widely applied for predicting prognosis and outcome in a clinical setting by combining multiple risk factors (35). In the present study, *CCNB1*, *CCNB2* and *FOXM1* were found to be predictors of LUAD. By combining the variables, a nomogram was then plotted. This nomogram appeared to be effective for in malignancy prediction with an AUC of 0.92, where it yielded superior findings in both external validation datasets, with AUCs of 0.91 and 0.96 for GSE10072 and GSE75037, respectively.

In the training set and validation set, all the AUC values of the present diagnostic model were >0.9. Therefore, according to this nomogram, the diagnostic evaluation of LUAD based on the expression levels of *CCNB1*, *CCNB2* and *FOXM1* yielded high accuracy and specificity. These three genes therefore have potential as biomarkers for the diagnosis of LUAD.

However, many limitations remain associated with the present study. Although the present study found that the higher expression of *CCNB1*, *CCNB2* and *CCNA2* is associated with poorer prognosis in LUAD, high expression of other cyclin family genes (CCNA2, CCNB1, CCNE1, CCNF and CCNJL) was associated with superior prognosis in colon cancer (64). Therefore, the prognostic impact of using the expression of genes in the cyclin family will likely be dependent on the type of tumors, which remains a topic of further study. In addition, the specific mechanistic role of these four hub genes on LUAD remain to be verified by *in vitro* or *in vivo* experiments.

In conclusion, in the present study bioinformatics analysis identified that *FOXM1*, *CCNB1*, *CCNB2* and *CCNA2* have hub genes that may the important for the development and prognosis of LUAD. In addition, the expression of these hub genes was found to be increased in Beas-2B and H1299 cell lines compared with those in the control cell line 16-HBE. Therefore, *CCNB1*, *CCNB2* and *FOXM1* may have potential diagnostic and prognostic value for LUAD in the future.

Acknowledgements

Not applicable.

Funding

No funding was received.

Availability of data and materials

The data generated and/or analyzed during the current study are available in the GEO database under accession number (GSE19188, GSE33532, GSE40791, GSE10072 and GSE75037) or at the following URLs: https://www.ncbi.nlm.nih.gov/geo/query/acc.cgi?acc=GSE19188; https://www.ncbi.nlm.nih.gov/geo/query/acc.cgi?acc=GSE33532; https://www.ncbi.nlm.nih.gov/geo/query/acc.cgi?acc=GSE40791; https://www.ncbi.nlm.nih.gov/geo/query/acc.cgi?acc=GSE10072;https://www.ncbi.nlm.nih.gov/geo/query/acc.cgi?acc=GSE75037.

Authors' contributions

XZ and XY confirm the authenticity of all the raw data. XZ provided the funding support of the study and designed this project. XY wrote the manuscript, and analyzed and interpreted the data. HG and ZT organized all the figures and interpreted data. YZ and PL performed tissue culture, RT-qPCR and western blot experiments, and revised the manuscript, figures and table. All authors read and approved the final manuscript.

Ethics approval and consent to participate

The present study was approved [approval no. KYLL-2020(KJ)P-0099] by the Medical Ethics Committee of the Second Hospital of Shandong University (Jinan, China). Written informed consent was obtained from all participants.

Patient consent for publication

Not applicable.

Competing interests

The authors declare that they have no competing interests.

References

1. Torre LA, Siegel RL and Jemal A: Lung cancer statistics. Adv Exp Med Biol 893: 1-19, 2016.
2. Boolell V, Alamgeer M, Watkins DN and Ganju V: The evolution of therapies in non-small cell lung cancer. Cancers (Basel) 7: 1815-1846, 2015.
3. Zenke Y, Tsuboi M, Chiba Y, Tsujino K, Satouchi M, Sawa K, Shimizu J, Daga H, Fujimoto D, Mori M, *et al*: Effect of second-generation vs third-generation chemotherapy regimens with thoracic radiotherapy on unresectable stage III non-small-cell lung cancer: 10-year follow-up of a WJTOG0105 phase 3 randomized clinical trial. JAMA Oncol 7: 904-909, 2021.
4. Min HY and Lee HY: Mechanisms of resistance to chemotherapy in non-small cell lung cancer. Arch Pharm Res 44: 146-164, 2021.
5. Lu X, Zhou D, Hou B, Liu QX, Chen Q, Deng XF, Yu ZB, Dai JG and Zheng H: Dichloroacetate enhances the antitumor efficacy of chemotherapeutic agents via inhibiting autophagy in non-small-cell lung cancer. Cancer Manag Res 10: 1231-1241, 2018.
6. Zhang Z, Zhang C, Yang Z, Zhang G, Wu P, Luo Y, Zeng Q, Wang L, Xue Q, Zhang Y, *et al*: m6A regulators as predictive biomarkers for chemotherapy benefit and potential therapeutic targets for overcoming chemotherapy resistance in small-cell lung cancer. J Hematol Oncol 14: 190, 2021.
7. Pang Z, Chen X, Wang Y, Wang Y, Yan T, Wan J and Du J: Comprehensive analyses of the heterogeneity and prognostic significance of tumor-infiltrating immune cells in non-small-cell lung cancer: Development and validation of an individualized prognostic model. Int Immunopharmacol 86: 106744, 2020.
8. Riess JW, Gandara DR, Frampton GM, Madison R, Peled N, Bufill JA, Dy GK, Ou SI, Stephens PJ, McPherson JD, *et al*: Diverse EGFR exon 20 insertions and co-occurring molecular alterations identified by comprehensive genomic profiling of NSCLC. J Thorac Oncol 13: 1560-1568, 2018.
9. Zhang F, Wang J, Ma M, Xu Y, Lu X and Wei S: Genomic alteration profiles of lung cancer and their relationship to clinical features and prognosis value using individualized genetic testing. J Thorac Dis 13: 5007-5015, 2021.
10. Jirawatnotai S, Dalton S and Wattanapanitch M: Role of cyclins and cyclin-dependent kinases in pluripotent stem cells and their potential as a therapeutic target. Semin Cell Dev Biol 107: 63-71, 2020.

11. Gong K, Zhou H, Liu H, Xie T, Luo Y, Guo H, Chen J, Tan Z, Yang Y and Xie L: Identification and integrate analysis of key biomarkers for diagnosis and prognosis of non-small cell lung cancer based on bioinformatics analysis. Technol Cancer Res Treat 20: 15330338211060202, 2021.
12. Thoma OM, Neurath MF and Waldner MJ: Cyclin-dependent kinase inhibitors and their therapeutic potential in colorectal cancer treatment. Front Pharmacol 12: 757120, 2021.
13. Susanti NMP and Tjahjono DH: Cyclin-dependent kinase 4 and 6 inhibitors in cell cycle dysregulation for breast cancer treatment. Molecules 26: 4462, 2021.
14. Hou J, Aerts J, den Hamer B, van Ijcken W, den Bakker M, Riegman P, van der Leest C, van der Spek P, Foekens JA, Hoogsteden HC, *et al*: Gene expression-based classification of non-small cell lung carcinomas and survival prediction. PLoS One 5: e10312, 2010.
15. Quek K, Li J, Estecio M, Zhang J, Fujimoto J, Roarty E, Little L, Chow CW, Song X, Behrens C, *et al*: DNA methylation intratumor heterogeneity in localized lung adenocarcinomas. Oncotarget 8: 21994-22002, 2017.
16. Zhang Y, Foreman O, Wigle DA, Kosari F, Vasmatzis G, Salisbury JL, van Deursen J and Galardy PJ: USP44 regulates centrosome positioning to prevent aneuploidy and suppress tumorigenesis. J Clin Invest 122: 4362-4374, 2012.
17. Gautier L, Cope L, Bolstad BM and Irizarry RA: Affy-analysis of Affymetrix GeneChip data at the probe level. Bioinformatics 20: 307-315, 2004.
18. Ritchie ME, Phipson B, Wu D, Hu Y, Law CW, Shi W and Smyth GK: limma powers differential expression analyses for RNA-sequencing and microarray studies. Nucleic Acids Res 43: e47, 2015.
19. Kolde R, Laur S, Adler P and Vilo J: Robust rank aggregation for gene list integration and meta-analysis. Bioinformatics 28: 573-580, 2012.
20. Yan S, Wang W, Gao G, Cheng M, Wang X, Wang Z, Ma X, Chai C and Xu D: Key genes and functional coexpression modules involved in the pathogenesis of systemic lupus erythematosus. J Cell Physiol 233: 8815-8825, 2018.
21. Sherman BT, Hao M, Qiu J, Jiao X, Baseler MW, Lane HC, Imamichi T and Chang W: DAVID: A web server for functional enrichment analysis and functional annotation of gene lists (2021 update). Nucleic Acids Res 50 (W1): W216-W221, 2022 (Epub ahead of print).
22. Yu G, Wang LG, Han Y and He QY: clusterProfiler: An R package for comparing biological themes among gene clusters. OMICS 16: 284-287, 2012.
23. Szklarczyk D, Morris JH, Cook H, Kuhn M, Wyder S, Simonovic M, Santos A, Doncheva NT, Roth A, Bork P, *et al*: The STRING database in 2017: Quality-controlled protein-protein association networks, made broadly accessible. Nucleic Acids Res 45 (D1): D362-D368, 2017.
24. Shannon P, Markiel A, Ozier O, Baliga NS, Wang JT, Ramage D, Amin N, Schwikowski B and Ideker T: Cytoscape: A software environment for integrated models of biomolecular interaction networks. Genome Res 13: 2498-2504, 2003.
25. Bader GD and Hogue CW: An automated method for finding molecular complexes in large protein interaction networks. BMC Bioinformatics 4: 2, 2003.
26. Assenov Y, Ramírez F, Schelhorn SE, Lengauer T and Albrecht M: Computing topological parameters of biological networks. Bioinformatics 24: 282-284, 2008.
27. Tang Z, Li C, Kang B, Gao G, Li C and Zhang Z: GEPIA: A web server for cancer and normal gene expression profiling and interactive analyses. Nucleic Acids Res 45 (W1): W98-W102, 2017.
28. Rouillard AD, Gundersen GW, Fernandez NF, Wang Z, Monteiro CD, McDermott MG and Ma'ayan A: The harmonizome: A collection of processed datasets gathered to serve and mine knowledge about genes and proteins. Database (Oxford) 2016: baw100, 2016.
29. Chandrashekar DS, Bashel B, Balasubramanya SAH, Creighton CJ, Ponce-Rodriguez I, Chakravarthi BVSK and Varambally S: UALCAN: A Portal for facilitating tumor subgroup gene expression and survival analyses. Neoplasia 19: 649-658, 2017.
30. Livak KJ and Schmittgen TD: Analysis of relative gene expression data using real-time quantitative PCR and the 2(-Delta Delta C(T)) method. Methods 25: 402-408, 2001.
31. Landi MT, Dracheva T, Rotunno M, Figueroa JD, Liu H, Dasgupta A, Mann FE, Fukuoka J, Hames M, Bergen AW, *et al*: Gene expression signature of cigarette smoking and its role in lung adenocarcinoma development and survival. PLoS One 3: e1651, 2008.
32. Girard L, Rodriguez-Canales J, Behrens C, Thompson DM, Botros IW, Tang H, Xie Y, Rekhtman N, Travis WD, Wistuba II, *et al*: An expression signature as an aid to the histologic classification of non-small cell lung cancer. Clin Cancer Res 22: 4880-4889, 2016.
33. Venables WN and Ripley BD: Modern applied statistics with S. 4th edition. Statistics and Computing, 2002.
34. Dobson AJ: An introduction to generalized linear models, second edition. Chapman & Hall/crc, 2001.
35. Harrell FE Jr: Regression modeling strategies: With applications to linear models, logistic regression, and survival analysis. Springer, 2010.
36. Robin X, Turck N, Hainard A, Tiberti N, Lisacek F, Sanchez JC and Müller M: pROC: An open-source package for R and S+ to analyze and compare ROC curves. BMC Bioinformatics 12: 77, 2011.
37. Eichhorn JM, Kothari A and Chambers TC: Cyclin B1 overexpression induces cell death independent of mitotic arrest. PLoS One 9: e113283, 2014.
38. Gavet O and Pines J: Progressive activation of CyclinB1-Cdk1 coordinates entry to mitosis. Dev Cell 18: 533-543, 2010.
39. Chang CC, Hung CM, Yang YR, Lee MJ and Hsu YC: Sulforaphane induced cell cycle arrest in the G2/M phase via the blockade of cyclin B1/CDC2 in human ovarian cancer cells. J Ovarian Res 6: 41, 2013.
40. Chu R, Terrano DC and Chambers TC: Cdk1/cyclin B plays a key role in mitotic arrest-induced apoptosis by phosphorylation of Mcl-1, promoting its degradation and freeing Bak from sequestration. Biochem Pharmacol 83: 199-206, 2012.
41. Ye C, Wang J, Wu P, Li X and Chai Y: Prognostic role of cyclin B1 in solid tumors: A meta-analysis. Oncotarget 8: 2224-2232, 2017.
42. Zhao P, Zhang P, Hu W, Wang H, Yu G, Wang Z, Li C, Bai J and Zhang Y: Upregulation of cyclin B1 plays potential roles in the invasiveness of pituitary adenomas. J Clin Neurosci 43: 267-273, 2017.
43. Chen EB, Qin X, Peng K, Li Q, Tang C, Wei YC, Yu S, Gan L and Liu TS: HnRNPR-CCNB1/CENPF axis contributes to gastric cancer proliferation and metastasis. Aging (Albany NY) 11: 7473-4791, 2019.
44. Zhang H, Zhang X, Li X, Meng WB, Bai ZT, Rui SZ, Wang ZF, Zhou WC and Jin XD: Effect of CCNB1 silencing on cell cycle, senescence, and apoptosis through the p53 signaling pathway in pancreatic cancer. J Cell Physiol 234: 619-631, 2018.
45. Sarafan-Vasseur N, Lamy A, Bourguignon J, Le Pessot F, Hieter P, Sesboüé R, Bastard C, Frébourg T and Flaman JM: Overexpression of B-type cyclins alters chromosomal segregation. Oncogene 21: 2051-2057, 2002.
46. Qian X, Song X, He Y, Yang Z, Sun T, Wang J, Zhu G, Xing W and You C: CCNB2 overexpression is a poor prognostic biomarker in Chinese NSCLC patients. Biomed Pharmacother 74: 222-227, 2015.
47. Lei CY, Wang W, Zhu YT, Fang WY and Tan WL: The decrease of cyclin B2 expression inhibits invasion and metastasis of bladder cancer. Urol Oncol 34: 237.e1-e10, 2016.
48. Li R, Jiang X, Zhang Y, Wang S, Chen X, Yu X, Ma J and Huang X: Cyclin B2 overexpression in human hepatocellular carcinoma is associated with poor prognosis. Arch Med Res 50: 10-17, 2019.
49. Wang X, Xiao H, Wu D, Zhang D and Zhang Z: miR-335-5p regulates cell cycle and metastasis in lung adenocarcinoma by targeting CCNB2. Onco Targets Ther 13: 6255-6263, 2020.
50. Lees EM and Harlow E: Sequences within the conserved cyclin box of human cyclin A are sufficient for binding to and activation of cdc2 kinase. Mol Cell Biol 13: 1194-1201, 1993.
51. Jiang P, Zhang M, Gui L and Zhang K: Expression patterns and prognostic values of the cyclin-dependent kinase 1 and cyclin A2 gene cluster in pancreatic adenocarcinoma. J Int Med Res 48: 300060520930113, 2020.
52. Brcic L, Heidinger M, Sever AZ, Zacharias M, Jakopovic M, Fediuk M, Maier A, Quehenberger F, Seiwerth S and Popper H: Prognostic value of cyclin A2 and B1 expression in lung carcinoids. Pathology 51: 481-486, 2019.

53. Ko E, Kim Y, Cho EY, Han J, Shim YM, Park J and Kim DH: Synergistic effect of Bcl-2 and cyclin A2 on adverse recurrence-free survival in stage I non-small cell lung cancer. Ann Surg Oncol 20: 1005-1012, 2013.
54. Li Z, Zhang Y, Zhou Y, Wang F, Yin C, Ding L and Zhang S: Tanshinone IIA suppresses the progression of lung adenocarcinoma through regulating CCNA2-CDK2 complex and AURKA/PLK1 pathway. Sci Rep 11: 23681, 2021.
55. Wang Y, Zhong Q, Li Z, Lin Z, Chen H and Wang P: Integrated profiling identifies CCNA2 as a potential biomarker of immunotherapy in breast cancer. Onco Targets Ther 14: 2433-2448, 2021.
56. Lee Y, Lee CE, Oh S, Kim H, Lee J, Kim SB and Kim HS: Pharmacogenomic analysis reveals CCNA2 as a predictive biomarker of sensitivity to polo-like kinase I inhibitor in gastric cancer. Cancers (Basel) 12: 1418, 2020.
57. Priller M, Pöschl J, Abrão L, von Bueren AO, Cho YJ, Rutkowski S, Kretzschmar HA and Schüller U: Expression of FoxM1 is required for the proliferation of medulloblastoma cells and indicates worse survival of patients. Clin Cancer Res 17: 6791-6801, 2011.
58. Liu B, Su F, Lin R, Teng H and Ju Y: Overexpression of forkhead box M1 is associated poor survival in patients with nonsmall cell lung cancer. J Cancer Res Ther 14 (Suppl): S1121-S1123, 2018.
59. Liang SK, Hsu CC, Song HL, Huang YC, Kuo CW, Yao X, Li CC, Yang HC, Hung YL, Chao SY, *et al*: FOXM1 is required for small cell lung cancer tumorigenesis and associated with poor clinical prognosis. Oncogene 40: 4847-4858, 2021.
60. Yi L, Wang H, Li W, Ye K, Xiong W, Yu H and Jin X: The FOXM1/RNF26/p57 axis regulates the cell cycle to promote the aggressiveness of bladder cancer. Cell Death Dis 12: 944, 2021.
61. Chen X, Müller GA, Quaas M, Fischer M, Han N, Stutchbury B, Sharrocks AD and Engeland K: The forkhead transcription factor FOXM1 controls cell cycle-dependent gene expression through an atypical chromatin binding mechanism. Mol Cell Biol 33: 227-236, 2013.
62. Li S, Liu N, Piao J, Meng F and Li Y: CCNB1 expedites the progression of cervical squamous cell carcinoma via the regulation by FOXM1. Onco Targets Ther 13: 12383-12395, 2020.
63. Chai N, Xie HH, Yin JP, Sa KD, Guo Y, Wang M, Liu J, Zhang XF, Zhang X, Yin H, *et al*: FOXM1 promotes proliferation in human hepatocellular carcinoma cells by transcriptional activation of CCNB1. Biochem Biophys Res Commun 500: 924-929, 2018.
64. Li J, Zhou L, Liu Y, Yang L, Jiang D, Li K, Xie S, Wang X and Wang S: Comprehensive analysis of cyclin family gene expression in colon cancer. Front Oncol 11: 674394, 2021.